

Optical Isolation using Compact Time-modulated Cavity Array

Adam Mock
 School of Engineering and Technology
 Central Michigan University
 Mount Pleasant, MI, USA
 mock1ap@cmich.edu

Abstract—It is shown using coupled mode theory and verified using finite-difference time-domain simulations how a time-modulated three-cavity array can be designed to allow transmission from port 1 to port 2 but to prevent transmission from port 2 to port 1 thereby implementing optical isolation. The reciprocity of the system is broken by phase-shifting the modulation signal applied to each cavity by 120 degrees which gives the system a synthetic linear momentum.

Index Terms—cavity resonators, finite-difference time-domain method, isolators, time-varying circuits.

I. INTRODUCTION

Optical isolators allow propagation of electromagnetic waves in one direction and block them in the reverse direction. To implement this functionality, the Lorentz reciprocity inherent in most materials must be broken. Most existing optical isolators use Faraday rotation induced by the magneto-optic effect. However, these devices can be bulky and require specialized magneto-optic materials which can be difficult to process in integrated photonics applications [1]. This work presents a theoretical framework verified by finite-difference time-domain simulation of an isolator device made by time-modulating the refractive index of three coupled cavities.

II. COUPLED CAVITIES

Fig. 1 (a) depicts a generic system comprised of two waveguides and three optical resonators with frequency ω_0 , cavity-coupling rate κ and waveguide coupling rate d . Temporal coupled mode theory (CMT) [2] can be used to model the dynamics of the system according to:

$$\dot{\mathbf{a}} = [-i\mathbf{\Omega} - \mathbf{\Gamma}]\mathbf{a} + 2\mathbf{D}^T \mathbf{s}_{\text{inc}}, \quad (1)$$

where $\mathbf{a} = [a_1(t) \ a_2(t) \ a_3(t)]^T$, $\mathbf{\Omega}$ is given by:

$$\mathbf{\Omega} = \begin{bmatrix} \omega_0 & \kappa & 0 \\ \kappa & \omega_0 & \kappa \\ 0 & \kappa & \omega_0 \end{bmatrix}, \quad (2)$$

$\mathbf{\Gamma}$ is given by:

$$\mathbf{\Gamma} = \begin{bmatrix} \gamma_i + \gamma_c & 0 & 0 \\ 0 & \gamma_i & 0 \\ 0 & 0 & \gamma_i + \gamma_c \end{bmatrix}, \quad (3)$$

and \mathbf{D} is given by:

$$\mathbf{D} = \frac{1}{2} \begin{bmatrix} d & 0 & 0 \\ 0 & 0 & 0 \\ 0 & 0 & d \end{bmatrix}. \quad (4)$$

$a_j(t)$ is the field amplitude in the j th resonator, γ_i is the intrinsic loss rate of an isolated resonator and γ_c is the loss rate of a resonator due to waveguide coupling. d and γ_c are related according to $d^2 = 2\gamma_c$. $\mathbf{s}_{\text{inc}} = [s_{i1} \ 0 \ s_{i2}]^T$ is a vector describing the incident field amplitudes in ports 1 and 2. The matrix \mathbf{D} has only two non-zero values consistent with only the left and right cavities being coupled to waveguides. The presence of only two coupling loss terms γ_c in $\mathbf{\Gamma}$ also reflects this configuration.

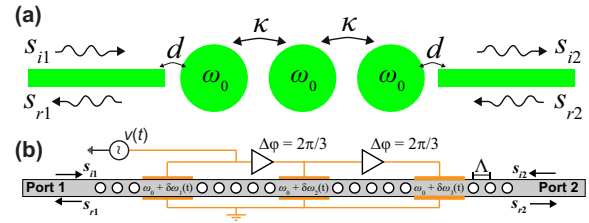


Fig. 1. (a) Schematic depiction of two coupled resonant cavities each of which is coupled to a waveguide. (b) Geometry of system modeled using FDTD. The index of the gray waveguide is set to 3.1. White areas are air. The time-variation of the refractive index was implemented within the FDTD algorithm rather than through an applied voltage as shown.

Fig. 1 (b) shows how the coupled-cavity system depicted in Fig. 1 (a) could be implemented in a compact integrated photonics platform. The gray region represents an InP rectangular waveguide. The cavities are defined by defects in a one-dimensional array of air holes etched into the semiconductor waveguide. The array of air holes creates a bandgap centered at the normalized frequency $\Lambda/\lambda_0 = 0.24$. When defects are introduced into the array, incident energy can couple into them, and the energy in the defects can then couple to output ports. Without modulation, the transmission spectra of this system would be the same for incidence from port 1 or 2.

Optical isolation is implemented by time-modulating the resonance frequency of each cavity via the electro-optic effect at a frequency ω_m which is much smaller than the optical carrier frequency. The sinusoidal signal applied to each cavity

is phase shifted by $2\pi/3$ resulting in a synthetic forward linear momentum applied to the system. It is this directional momentum that breaks the reciprocity necessary for isolation.

In the presence of the proposed time-modulation, the CMT equation becomes:

$$\dot{\mathbf{a}} = [-i\mathbf{\Omega} - i\delta\mathbf{\Omega}(t) - \mathbf{\Gamma}]\mathbf{a} + 2\mathbf{D}^T \mathbf{s}_{\text{inc}}, \quad (5)$$

where $\delta\mathbf{\Omega}(t)$ is given by:

$$\delta\omega \begin{bmatrix} \cos(\omega_m t) & 0 & 0 \\ 0 & 2 \cos(\omega_m t + 2\pi/3) & 0 \\ 0 & 0 & \cos(\omega_m t + 4\pi/3) \end{bmatrix}. \quad (6)$$

To obtain the scattered wave amplitude into ports 1 and 2 one solves Eq. 5 for a_j and substitutes the result into:

$$\mathbf{s}_{\text{ref}} = -\mathbf{s}_{\text{inc}} + \mathbf{D}\mathbf{a}, \quad (7)$$

where $\mathbf{s}_{\text{ref}} = [s_{r1} \ 0 \ s_{r2}]^T$ represents the amplitudes of the outgoing waves in ports 1 and 2 [2].

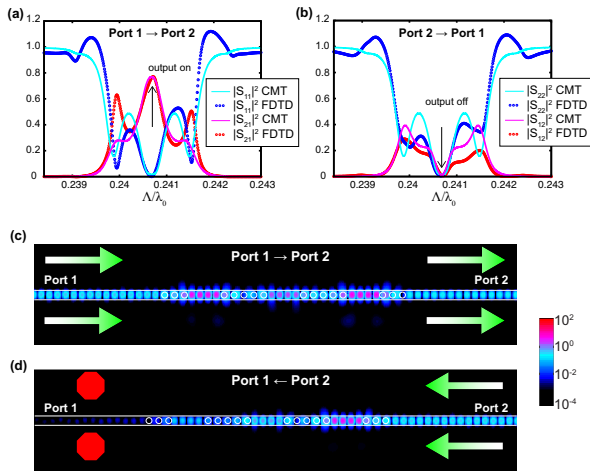


Fig. 2. (a) The scattering parameters calculated using CMT and simulated using FDTD for incidence from port 1. (b) The scattering parameters for incidence from port 2. (c) Depiction of $|H_z(x, y)|^2$ on a logarithmic scale for incidence from port 1 at the isolation frequency. The field is shown radiating into port 2. (d) Same as (c) except incident energy is from port 2, and the energy is blocked from reaching port 1.

Figs. 2 (a) and (b) depict the scattering spectra for incidence from ports 1 and 2, respectively, calculated using CMT and simulated via the two-dimensional finite-difference time-domain (FDTD) method. The resonance frequencies of the three-cavity system are ω_0 and $\omega_0 \pm \sqrt{2}\kappa$. The three peaks in the transmission spectra $|S_{21}|^2$ correspond to the three resonance frequencies. The system was designed to provide optical isolation at the middle resonance frequency (ω_0) at a normalized frequency $\omega_0\Lambda/(2\pi c) = \Lambda/\lambda_0 = 0.2407$. The modulation parameters were set to $\omega_m = 0.00082$ and $\delta\omega = 0.0046$ which were determined using a numerical optimization that simultaneously maximized (minimized) throughput in the forward (backward) direction based on the CMT equations [3]. The qualitative agreement between the theoretical predictions and the numerical simulation is good. Figs. 2 (a) and (b) show

how the transmission is on in the forward direction and off in the backward direction. In both cases, the reflected energy is minimal at the isolation frequency. Figs. 2 (c) and (d) depict the fields in the cases of incidence in the forward and backward directions, respectively, and confirm the isolation behavior of the device. We found that with the phase-shifted spatio-temporal modulation scheme and appropriately chosen values of $\delta\omega$ and ω_m , the power transmission from port 1 to port 2 is 77%, and the power transmission from port 2 to port 1 is suppressed to 0.7% resulting in 20.4dB of isolation. Using intuition from our previous studies [3], [4], we believe the transmission can be further increased and the required modulation frequency and amplitude decreased by using cavities with lower intrinsic losses (γ_i). The intrinsic loss of the proposed cavities can be decreased using straight-forward geometry modifications [5].

III. ANALYSIS OF TIME-VARYING SYSTEMS

In the solution of the CMT equations in the presence of modulation, one must introduce the ansatz $a_j(t) = \sum_n a_{j,n} e^{-i(\omega+n\omega_m)t}$ and solve for the Fourier series coefficients $a_{j,n}$. In order to keep the analysis reasonable, we truncated the Fourier series and kept only the $n = -1, 0, 1$ harmonics. Even with this approximation, the qualitative agreement between the theoretical predictions and FDTD simulation is good.

The FDTD simulation is performed by exciting the system with a pulse centered at the frequency of interest. The incident, reflected and transmitted power spectra are recorded. $|S_{11}|^2$ and $|S_{21}|^2$ are obtained by dividing the reflected and transmitted power spectra by the incident power spectra ($|S_{12}|^2$ and $|S_{22}|^2$ are obtained analogously). This excitation energizes a range of frequencies simultaneously thereby producing entire scattering spectra with a single simulation. In the presence of time-varying materials, the scattering spectra will display frequency mixing. In Figs. 2 (a) and (b) the reflected scattering parameter exceeds 1 due to overlapping of multiple sidebands. In another presentation [6], we discuss more details of time-domain modeling of time-varying materials.

REFERENCES

- [1] Y. Shoji, T. Mizumoto, H. Yokoi, I-W. Hsieh, and R. M. Osgood, "Magneto-optical isolator with silicon waveguide fabricated by direct bonding," *Applied Physics Letters*, vol. 92, pp. 071117, 2008.
- [2] W. Suh, Z. Wang, and S. Fan, "Temporal coupled-mode theory and the presence of non-orthogonal modes in lossless multimode cavities," *IEEE Journal of Quantum Electronics*, vol. 40, pp. 1511–1518, 2004.
- [3] A. Mock, D. Sounas, and A. Alù, "Magnet-Free Circulator Based on Spatiotemporal Modulation of Photonic Crystal Defect Cavities," *ACS Photonics*, vol. 6, pp. 2056–2066, 2019.
- [4] A. Mock, D. Sounas, and A. Alù, "Tunable orbital angular momentum radiation from angular-momentum-biased microcavities," *Physical Review Letters*, vol. 121, pp. 103901, 2018.
- [5] A. Zain, N. Johnson, M. Sorel, and R. De La Rue, "Ultra high quality factor one dimensional photonic crystal/photonic wire micro-cavities in silicon-on-insulator (SOI)," *Optics Express*, vol. 16, pp. 12084, 2008.
- [6] A. Mock, "Calculating Scattering Spectra using Time-domain Modeling of Time-modulated Systems," submitted to 2020 International Applied Computational Electromagnetics (ACES) Symposium, Monterey, CA, USA, March 2020, paper 1140.